Cover Page

15th International ASTM/ESIS Symposium on Fatigue and Fracture Mechanics

(40th National Symposium on Fatigue and Fracture Mechanics)

May 20-22, 2015, Anaheim, CA

Experimental and Finite Element Modeling of Near-Threshold Fatigue Crack Growth for the K-Decreasing Test Method

Stephen W. Smith, NASA Langley Research Center, Hampton, VA, USA

Banavara R. Seshadri, National Institute of Aerospace, Hampton, VA, USA

John A. Newman, NASA Langley Research Center, Hampton, VA, USA

Abstract Summary (one paragraph 300 hundred max)

The experimental methods to determine near-threshold fatigue crack growth rate data are prescribed in ASTM standard E647. To produce near-threshold data at a constant stress ratio (R), the applied stress-intensity factor (K) is decreased as the crack grows based on a specified K-gradient. Consequently, as the fatigue crack growth rate threshold is approached and the crack tip opening displacement decreases, remote crack wake contact may occur due to the plastically deformed crack wake surfaces and shield the growing crack tip resulting in a reduced crack tip driving force and non-representative crack growth rate data. If such data are used to life a component, the evaluation could yield highly non-conservative predictions. Although this anomalous behavior has been shown to be affected by K-gradient, starting K level, residual stresses, environmental assisted cracking, specimen geometry, and material type, the specifications within the standard to avoid this effect are limited to a maximum fatigue crack growth rate and a suggestion for the K-gradient value. This paper provides parallel experimental and computational simulations for the K-decreasing method for two materials (an aluminum alloy, AA 2024-T3 and a titanium alloy, Ti 6-2-2-2-2) to aid in establishing clear understanding of appropriate testing requirements. These simulations investigate the effect of K-gradient, the maximum value of stress-intensity factor applied, and material type. A material independent term is developed to guide in the selection of appropriate test conditions for most engineering alloys. With the use of such a term, near-threshold fatigue crack growth rate tests can be performed at accelerated rates, near-threshold data can be acquired in days instead of weeks without having to establish testing criteria through trial and error, and these data can be acquired for most engineering materials, even those that are produced in relatively small product forms.

(Extended-Abstract – not to exceed 8 pages)

INTRODUCTION:

ASTM Standard E647 [1] prescribes the test specifications for the development of fatigue crack growth rate data. To evaluate the near-threshold behavior for a material at constant stress ratio (R), a K-decreasing test method is prescribed. Here, the near-threshold regime is determined by first precracking a specimen and slowly reducing the applied stress-intensity factor (K) as defined by the K-gradient (C),

$$C = \frac{dK/da}{K}; \quad (1)$$

such that K, here used to represent the cyclic stress-intensity factor range, ΔK, maximum K, K_{max}, or minimum K, K_{min}, is reduced as the crack length (a) increases. The standard prescribes that a value of C equal to or greater than -0.08 mm^{-1} (-2 in^{-1}) should be used to preclude anomalous results. This limitation on K-gradient was determined based on the data available during the development of the standard [2]. In addition to suggesting a limitation on the K-gradient, the standard prescribes that a maximum fatigue crack growth rate (da/dN_{max}) of $1x10^{-8}$ m/cycle ($4x10^{-7}$ in/cycle) should not be exceeded during a K-decreasing test. This additional constraint was placed on the testing as it was observed that transient behavior is more likely to occur for higher applied stress-intensity factors. While these limitations for C and da/dN_{max} were consistent with the available data, they are not based on direct scientific principles.

It has been shown that results for K-decreasing tests are influenced by the value of K-gradient, starting K level, residual stresses, environmental issues, specimen geometry, and material type [2-6]. Experimental and analytical results suggest that during a K-decreasing procedure artificially high threshold values can be obtained as the value of C is decreased or the maximum K is increased [3-4, 7-10] as closure of the plastically deformed crack wake remote from the growing crack tip shields the crack tip, reducing the crack tip driving force. Here, the use of large K-gradients (small values of C) and high initial values of K_{max} (often exceeding da/dN_{max} prescribed in E647 [1]) were found to produce anomalous results. These results suggest that the limitations specified in E647 are often too restrictive [3-4] resulting in overly long testing times and requiring the growth of relatively long cracks, which can be difficult if the material form limits specimen size. However, other researchers [11] have suggested that since the K-decreasing method can produce anomalous results under certain conditions, alternate approaches to determine near threshold data should be sought.

While there have been several studies examining the effect of K-decreasing test conditions on the measured fatigue crack growth rate in the near-threshold regime, there has not been a systematic study with direct comparison of experimental and computational simulations to evaluate the various parameters that can affect the K-decreasing test method for multiple materials. This study examines the effects of K-gradient, $K_{max,i}$ and material (aluminum alloy 2024-T3 and a $\alpha+\beta$ titanium alloy Ti 6-2-2-2-2), to evaluate if material independent test specifications can be realized for the K-decreasing test method. These results should assist in developing a physical understanding of the remote closure effects during K-decreasing tests and provide initial understanding to define if alternate K-decreasing test methods, such as the CK^2 approach [12] should be used instead of the K-gradient approach.

(Extended-Abstract – not to exceed 8 pages)

TEST METHOD/OVERVIEW

Fatigue crack growth rate tests were performed using the K-decreasing method detailed in ASTM standard E647 [1] using two materials, aluminum alloy 2024-T3 and titanium alloy Ti 6-2-2-2-2. These materials were chosen since previous studies [13-14] have indicated that these materials are relatively well behaved (cracks grow relatively straight, the fracture surfaces are not rough and the oxides that grow on the surfaces in room temperature laboratory air are not voluminous) and are free of residual stress, allowing this study to isolate the effects of plasticity induced closure with limited roughness and oxide induced closure. Additionally, these materials have very different mechanical properties (σ_y (AA2024-T3) ≈ 345 MPa (50.0 ksi), σ_y (Ti 6-2-2-2-2) ≈ 1120 MPa (162 ksi)) to evaluate the effect of testing conditions for different materials. Potential effects of specimen geometry were not studied as all tests were performed using eccentrically loaded single edge tension (ESE(T)) specimens as detailed in E647 [1]. Both materials were sheet products and specimens were machined with the loading axis parallel to the rolling direction and the specimen thickness was the same as the respective sheet product. AA 2024 specimens were 2.3 mm (0.091 inch) thick and 38 mm (1.5 inch) wide and the Ti 6-2-2-2-2 specimens were 1.6 mm (0.063 inch) thick and 38 mm (1.5 inch) wide. All K-decreasing tests were performed for R = 0.1. Cyclic loading was performed at 10 Hz for the AA 2024 tests and 5 Hz for the Ti 6-2-2-2-2 tests. The K-decreasing tests were performed for several values of $K_{max,i}$ and for values of C from -0.08 mm^{-1} (-2 in^{-1}) to -2.36 mm^{-1} (-60 in^{-1}).

Computational simulations were performed using three-dimensional elastic-plastic finite element software, ZIP3D [15], to model plasticity-induced crack closure under cyclic loading [5-6, 9-10, 16-18]. Crack closure and ΔCTOD estimates were made by monitoring nodal displacements during the loading and unloading portions of the cyclic loading. Closure estimates are performed at both "local" and "remote" locations for each simulation. The "local" location represents a node very close to the simulated crack tip. The "remote" location represents the start of the K-decreasing simulation or the application of $K_{max,i}$. Closure levels were evaluated at the outer surface and midline of the specimen. The ESE(T) specimen has two planes of symmetry, making it necessary to only model one fourth of the total specimen. A typical model consisting of 48,102 nodes and 30,520 elements is shown in Figure 1. The crack tip elements were on the order of 10 microns in length. Typical stress-strain curves for each material were used. Small deformation theory was employed and the crack front was advanced one element during each cycle such that da = 10 μm. Load cycles were applied to simulate K-decreasing tests for several values of $K_{max,i}$ and C consistent with the experimental tests. All simulations were performed for the entire range of the K-decreasing test from ΔK at $K_{max,i}$ to ΔK=1 MPa√m, to insure the simulations were performed past the expected threshold value (typically around 3 MPa√m for both of these materials at R = 0.1).

RESULTS/DISCUSSION

Six K-decreasing tests using different testing conditions were examined for the AA 2024-T3 material, with $K_{max,i}$ applied being either 5.44 MPa√m or 11.0 MPa√m. Plots of the fatigue crack growth rate versus applied ΔK data are shown in Figure 2 on a typical log-log plot. Here, the four tests initiated at $K_{max,i}$ = 5.44 MPa√m satisfied the limitation of $da/dN_{max} \leq 1 \times 10^{-8}$ m/cycle from

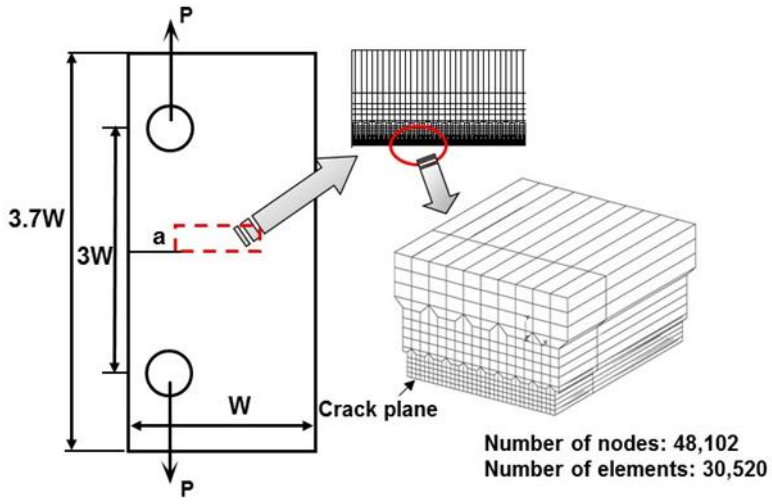

Figure 1. A typical ZIP3D finite element mesh for the ESE(T) specimen.

E647 [1], while the two tests initiated at $K_{max,i}$ = 11.0 MPa√m grew at an initial rate more than 1 order of magnitude greater than that suggested in the standard. Sixteen K-decreasing tests using different testing conditions were examined for the Ti 6-2-2-2-2 material, with values of $K_{max,i}$ applied of 4.95 MPa√m, 12.1 MPa√m, 16.5 MPa√m, or 22.0 MPa√m. Plots of fatigue crack growth rate versus ΔK for seven of these tests are shown in Figure 3. Only the tests initiated at $K_{max,i}$ = 4.95 MPa√m satisfied the limitation of $da/dN_{max} \leq 1 \times 10^{-8}$ m/cycle from E647 [1]. For each of the K-decreasing tests, ΔK_{th} was evaluated at da/dN = $1x10^{-10}$ m/cycle consistent with the

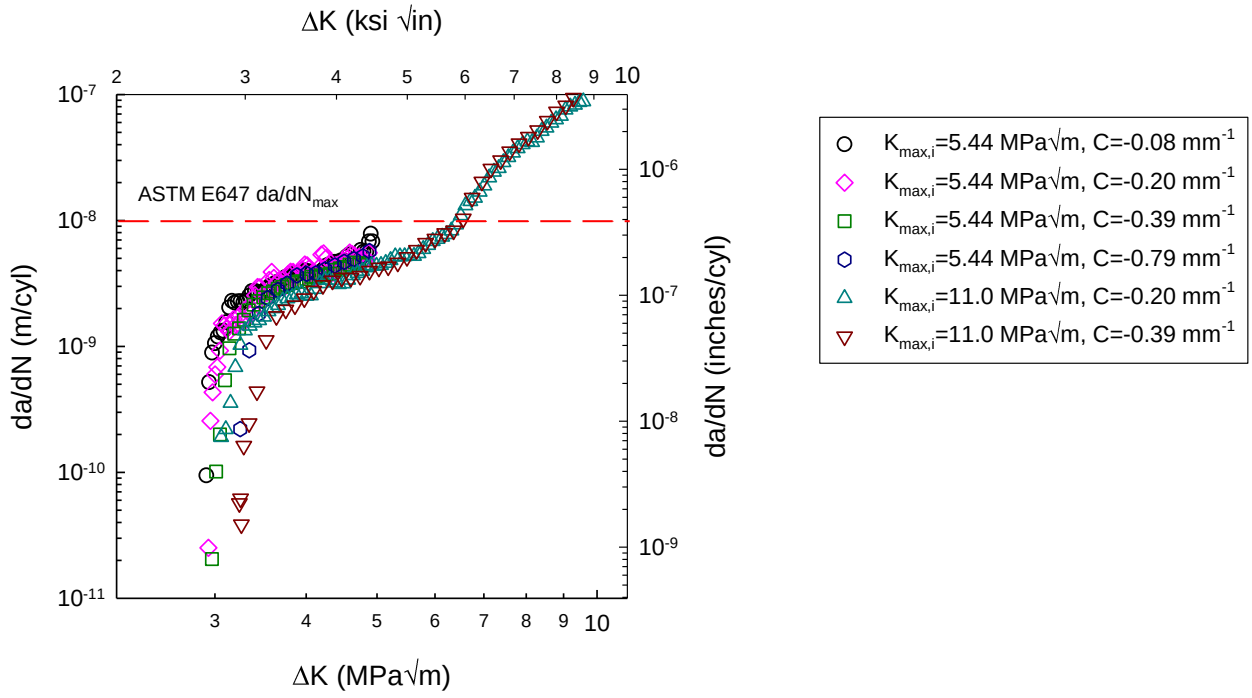

Figure 2. Near-threshold fatigue crack growth rate curves for AA 2024-T3 R = 0.1 at various values of C and $K_{max,i}$.

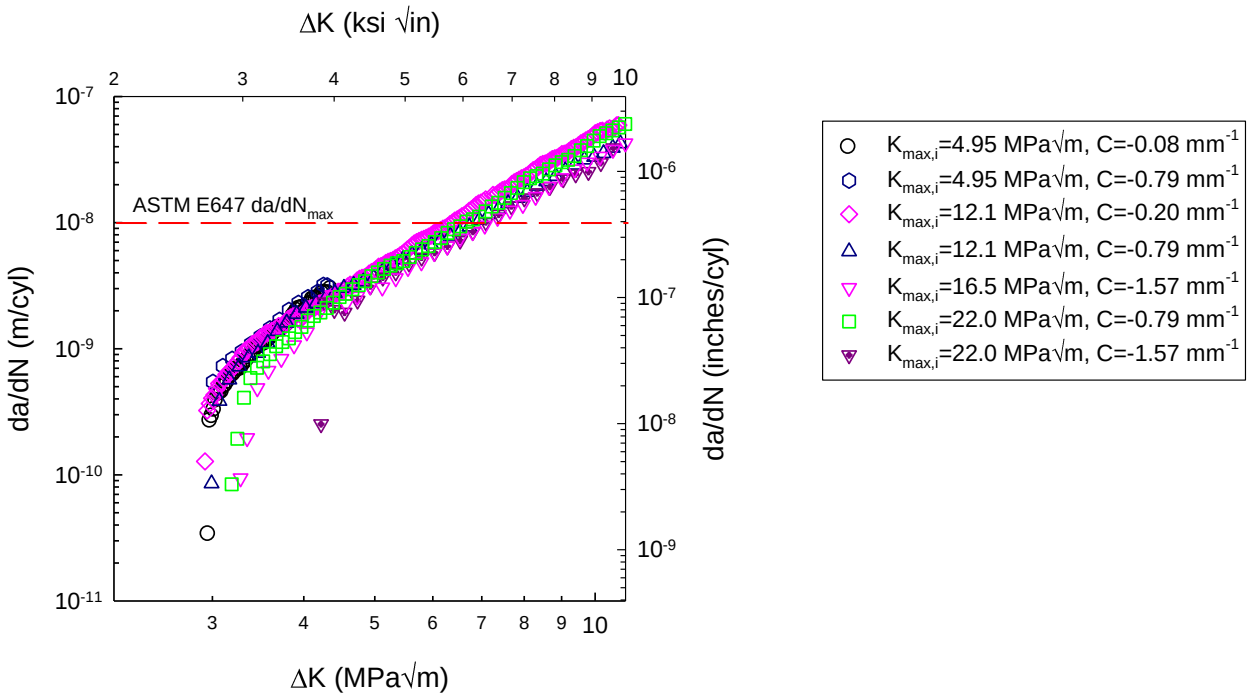

Figure 3. Near-threshold fatigue crack growth rate curves for Ti 6-2-2-2-2 R = 0.1 at various values of C and $K_{max,i}$.

methods described in E647 [1]. These results are summarized for AA 2024 in Table 1 and Ti 6-2-2-2-2 in Table 2. Symbols (* and #) are also supplied in Tables 1 and 2 to represent results for the computational simulations, which will be discussed in the following paragraph. While several of the values of ΔK_{th} for AA 2024 are in very good agreement, two of the tests ($K_{max,i}$ = 5.44 MPa√m, C=-0.79 mm^{-1} and $K_{max,i}$ = 11.0 MPa√m, C=-0.39 mm^{-1}) resulted in slightly greater values. For Ti 6-2-2-2-2, three of the tests ($K_{max,i}$ = 16.5 MPa√m, C=-1.57 mm^{-1} and $K_{max,i}$ = 22.0 MPa√m, C=-0.79 mm^{-1} and -1.57 mm^{-1}) resulted in higher values of ΔK_{th}. The higher values of ΔK_{th} suggest remote closure is occurring and the measured values of ΔK_{th} are not accurate.

Table 1. ΔK_{th} values for AA 2024 K-decreasing tests at various values of C and $K_{max,i}$.

C(mm^{-1}) [in^{-1}]	$K_{max,i}$ = 5.44 MPa√m	$K_{max,i}$ = 11 MPa√m
-0.08 [-2]	2.90 MPa√m	---
-0.20 [-5]	2.95 MPa√m	3.01 MPa√m *
-0.39 [-10]	3.03 MPa√m	3.29 MPa√m *
-0.79 [-20]	3.20 MPa√m	---

* remote closure determined by computational simulation

Table 2. ΔK_{th} values for Ti 6-2-2-2-2 K-decreasing tests at various values of C and $K_{max,i}$.

C(mm^{-1}) [in^{-1}]	$K_{max,i}$ = 4.95 MPa√m	$K_{max,i}$ = 12.1 MPa√m	$K_{max,i}$ = 16.5 MPa√m	$K_{max,i}$ = 22.0 MPa√m
-0.08 [-2]	2.95 MPa√m	---	---	---
-0.20 [-5]	2.68 MPa√m #	2.88 MPa√m #	--- #	--- *
-0.39 [-10]	2.70 MPa√m #	--- #	--- #	2.68 MPa√m *
-0.79 [-20]	2.67 MPa√m #	2.98 MPa√m #	2.59 MPa√m *	3.18 MPa√m *
-1.18 [-30]	2.78 MPa√m	---	2.64 MPa√m	---
-1.57 [-40]	--- #	2.95 MPa√m #	3.22 MPa√m *	3.56 MPa√m *
-1.95 [-50]	---	2.85 MPa√m	---	---
-2.36 [-60]	---	2.90 MPa√m	---	---

* remote closure determined by computational simulation

\# no remote closure determined by computational simulation

Computational results for two testing conditions for the AA 2024 material are shown in Figure 4. The results are presented as crack closure level (represented as the load at which closure is identified normalized by the maximum applied load during the cycle, P_{cl}/P_{max}) versus ΔK for the "local" and "remote" locations. For all simulations, closure at the outer surface was found to be greatest and is presented here. Figure 4 indicates that remote closure is operative for both test conditions presented. For C= -0.39 mm^{-1}, as the applied ΔK is decreased from the initial value of 9.9 MPa√m, the closure level at the "local" location decreases while the closure level at the "remote" location increases. These results indicate that for applied ΔK > 6 MPa√m, the crack behaves as expected with the crack wake just behind the crack tip closing first (i.e. greater value of P_{cl}/P_{max}) with the wake closing as load is further reduced. However, for applied ΔK < 5.5 MPa√m, the "remote" location will close first, shielding the crack tip and resulting in a reduced crack tip driving force and anomalous near-threshold behavior. For C= -0.20 mm^{-1}, similar results are indicated with the "remote" location closing first for ΔK< 3.3 MPa√m. However, since this value is so close to the observed ΔK_{th} (3.01 MPa√m), little effect of this remote closure is expected. Here, it is shown that for the same value of $K_{max,i}$, remote closure is exacerbated for increasing C. A total of two test conditions were evaluated for the AA 2024 material and fourteen conditions for the Ti 6-2-2-2-2 material. These results are summarized in Tables 1 and 2 where the # symbols represent analyses where no remote closure was observed and the * symbols represent analyses where remote closure was observed at some point during the simulation. For the five experimental conditions that were observed to result in significantly higher values of ΔK_{th}, computational simulations were performed for four of these conditions and all four simulations indicated remote closure. For an additional three simulations which indicated remote closure very close to the measured ΔK_{th} value, the experimental results did not suggest remote closure however, indicating that any influence of remote closure is very small.

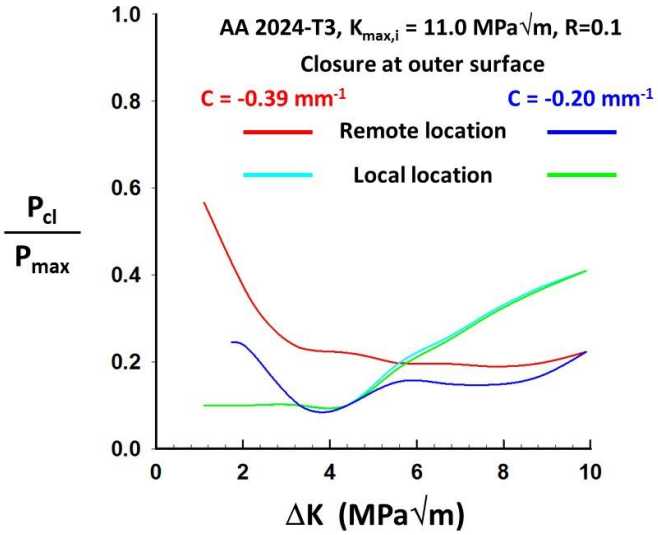

Figure 4. Comparison of remote and local closure levels for AA 2024-T3 $K_{max,i}$= 11.0 MPa√m and R=0.1 at outer surface for C=-0.39 and -0.20 mm^{-1}.

In this study, three test variables were examined 1) K-gradient, 2) $K_{max,i}$ and 3) material type. To evaluate the effect of these variables, the data for both materials are plotted in Figure 5 as normalized ΔK_{th} versus log(–C $(K_{max,i}/ \sigma_y)^2$). Here, the results for all twenty-two experimental tests are plotted. The value of $\Delta K_{th,baseline}$ for the AA 2024 material was taken to be 2.90 MPa√m, which was the result for $K_{max,i}$ = 5.44 MPa√m and C= -0.08 mm^{-1}; for Ti 6-2-2-2-2, $\Delta K_{th,baseline}$ was taken to be 2.80 MPa√m, which was the average of $K_{max,i}$ = 4.95 MPa√m, C= -0.08, -0.20 and -0.39 mm^{-1} and $K_{max,i}$ = 12.1 MPa√m, C= -0.20 mm^{-1}. The thirteen simulations which were performed using identical parameters as those of the experimental tests are also represented in Figure 5 by filling the symbols either black to indicate that no remote closure was observed or red to indicate that remote closure was observed in the simulation. In Figure 5, dashed red lines of ± 7.5% deviation for the normalized ΔK_{th} are included to indicate scatter in the values of ΔK_{th}. Of the twenty-two experimental tests, five tests resulted in a measured value greater than this scatter band, with the value of $-C(K_{max,i} / \sigma_y)^2$ being greater or equal to 0.196 for each case. For four of these test conditions, computational simulations were also performed and in each of these simulations remote closure was observed well above the measured ΔK_{th}. An additional three simulations revealed remote closure for parameters where tests were also performed. Each of these three simulations indicated remote closure very close to the measured valued of ΔK_{th} and while the experimental results did not appear to be adversely affected, this must be considered when evaluating conditions for a reliable test standard. Here, the lowest value of $-C(K_{max,i} / \sigma_y)^2$ indicating remote closure where an experimental measurement was also made was equal to 0.154. By examining results for several different materials under varying test conditions, it is believed that reliable, material dependent, test limitations for the K-decreasing test method can be determined. The results in Figure 5 would suggest that a value of $-C(K_{max,i} / \sigma_y)^2$ less than 0.1 should result in reliable results for a K-decreasing test. By using this relationship, one can determine the minimum value of C for any material for a specific value of $K_{max,i}$. Similar data can be acquired for the CK^2 test approach to determine a minimum value of C_i for any material for a specific value of $K_{max,i}$. Future tests and computational simulations will be performed to evaluate this test approach.

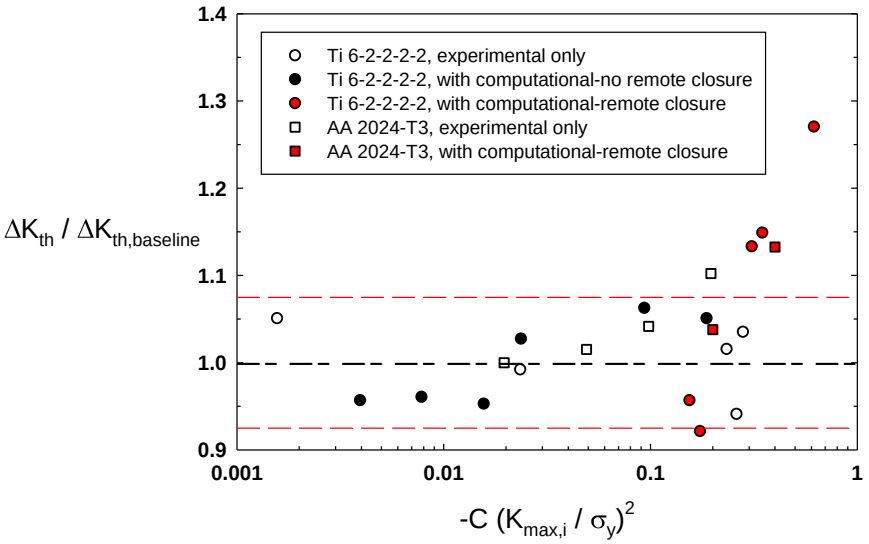

Figure 5. Normalized threshold value versus a dimensionless K-decreasing parameter for AA 2024 and Ti 6-2-2-2-2 experimental and computational results for K-decreasing tests at R=0.1.

CONCLUSIONS

Experimental tests and computational simulations were performed to assess the effects of K-gradient, $K_{max,i}$ and material type on the results of a K-decreasing test in the near threshold regime using the method detailed in ASTM standard E647 [1]. This study was designed to specifically examine the effects of plasticity induced remote closure on the K-decreasing test method and it should be noted that materials with significant roughness or oxide induced closure may be more adversely affected by testing at lower values of C or higher $K_{max,i}$.

- The suggested test limitations for K-gradient and da/dN_{max} in ASTM standard E647 are shown to be overly conservative for the two materials examined in this study. The effect of K-gradient and $K_{max,i}$ was found to be material dependent and therefore may not be conservative for materials that are much lower in strength than those examined in this study.
- Experimental tests and computational simulations of the K-decreasing test method are in very good agreement and further support the argument that remote closure can adversely affect near-threshold crack growth behavior for certain test conditions.
- A material independent term $(-C(K_{max,i} / \sigma_y)^2)$ has been shown to be appropriate to determine reliable values of K-gradient and $K_{max,i}$ for both of the materials examined in this study.

ACKNOWLEDGEMENTS

The authors have had valuable conversations with many members of ASTM Committee E08 that have significantly affected this work. Collaborations with four specific members are particularly noteworthy: Keith Donald of Fracture Technology Associates, Mark James of Alcoa Technical Center, Keith Kersey of Pratt & Whitney and Rick Pettit of FractureLab.

REFERENCES

1. ASTM: Standard Test Method for Measurement of Fatigue Crack Growth Rates, E647-13, 2013.
2. S.J. Hudak Jr., et al., "Development of Standard Methods of Testing and Analyzing Fatigue Crack Growth Rate Data," AFML TR 78-40, Air Force Materials Laboratory, Wright Patterson Air Force Base, OH, 1978.
3. R.W. Bush, J.K. Donald, R.J. Bucci, "Pitfalls to Avoid in Threshold Testing and its Interpretation," *Fatigue Crack Growth Thresholds, Endurance Limits, and Design, ASTM STP 1372*, J.C. Newman Jr., R.S. Piascik, eds., ASTM, West Conshohocken, PA, pp. 269-284, 2000.
4. J.W. Sheldon, K.R. Bain, J.K. Donald "Investigation of the Effects of Shed-Rate, Initial K_{max}, and Geometric Constraint on ΔK_{th} in Ti-6Al-4V at Room Temperature" *Int. Journal of Fatigue*, Vol. 21, pp. 733-741, 1999.
5. R.C. McClung, "The Influence of Applied Stress, Crack Length, and Stress Intensity Factor on Crack Closure", *Metallurgical Transactions A*, Vol. 22A, pp. 1559-1571, July 1991.
6. B.R. Seshadri, S.W. Smith, "Three Dimensional Constraint Effects on the Estimated ΔCTOD During Numerical Simulation of Different Fatigue Threshold Testing Techniques," 48th AIAA/ASME/AHS/ASC Structures, Structural Dynamics, and Materials Conference, April 23-26, 2007.
7. J.K. Donald, P.C. Paris "An Evaluation of K Estimation Procedures on 6061-T6 and 2024-T3 Aluminum Alloys," *Proceedings of Fatigue Damage of Structural Materials II*, 1998.
8. K. Minakawa, J.C. Newman Jr., A.J. McEvily, "A Critical Study of the Closure Effect on Near-Threshold Fatigue Crack Growth," *Fatigue and Fracture of Engineering Materials and Structures*, Vol. 6, pp. 359-365, 1983.
9. R.C. McClung "Analysis of Fatigue Crack Closure During Simulated Threshold Testing," *Fatigue Crack Growth Thresholds, Endurance Limits, and Design, ASTM STP 1372*, J.C. Newman Jr., and R.S. Piascik, eds., ASTM, West Conshohocken, PA, pp. 209-226, 2000.
10. R.C. McClung, "Finite Element Modeling of Crack Closure During Simulated Fatigue Threshold Testing," *Int. Journal of Fracture*, Vol. 52, pp. 145-157, 1991.
11. J.C. Newman Jr., Y. Yamada, "Compression Precracking Methods to Generate near-Threshold Fatigue-Crack-Growth-Rate Data," *Int. Journal of Fatigue*, Vol. 32, pp. 879-885, 2010.
12. R.G. Pettit, J.A. Newman, J.D. Hochhalter, J.K. Donald, "Shed Rate Effects, and a New Axisymmetric Specimen for Crack Growth Threshold Testing," 13th International ASTM/ESIS Symposium on Fatigue and Fracture Mechanics, Nov. 13-15, 2013.
13. J.A. Newman, W.T. Riddell, R.S. Piascik, "Effects of K_{max} on Fatigue Crack Growth Threshold in Aluminum Alloys," *Fatigue Crack Growth Thresholds, Endurance Limits, and Design, ASTM STP 1372*, J.C. Newman Jr., and R.S. Piascik, eds., ASTM, West Conshohocken, PA, pp. 63-77, 2000.
14. S.W. Smith, R.S. Piascik. "Fatigue Crack Growth Characteristics of Thin Sheet Titanium Alloy Ti 6-2-2-2-2," NASA / TM-2001-210830, March 2001.
15. K.N. Shivakumar, J.C. Newman Jr., "ZIP3D- An Elastic-Plastic Finite Element Analysis Program for Cracked Bodies, NASA TM-1990-102753, November 1990.
16. S.R. Daniewicz, S.D. Skinner, "Finite Element Analysis of Fatigue Crack Growth Threshold Testing Techniques," 13th European Conference on Fracture, (ECF13), 2000.
17. B.R. Seshadri, S.C. Forth, "Finite Element Simulation and Estimation of Cyclic Crack Tip Opening Displacement for Different Specimens During Fatigue Threshold Testing," 5th International ASTM/ESIS Symposium on Fatigue and Fracture Mechanics, May 16-19, 2005.
18. B.R. Seshadri, S.C. Forth, "Numerical Simulation and Evaluation of Different Fatigue Threshold Testing Techniques," 9th International Fatigue Congress, May 14-19, 2006.